frontiers | Frontiers in Earth Science

TYPE Original Research
PUBLISHED 22 February 2024
DOI 10.3389/feart.2024.1322495

OPEN ACCESS

EDITED BY
Jianyong Han,
Shandong Jianzhu University, China

REVIEWED BY
Qing Ma,
Tsinghua University, China
Yubing Gao,
China University of Mining and Technology, Beijing, China
Tianran Ma,
China University of Mining and Technology, China
Hamdi Omar,
Ghent University, Belgium

*CORRESPONDENCE
Juan Jin,
jinjuan022@petrochina.com.cn
Weixi Chen,
chenwxqh@petrochina.com.cn

RECEIVED 16 October 2023
ACCEPTED 05 February 2024
PUBLISHED 22 February 2024

CITATION
Jin J, Liu J, Chen W, Li G, Cheng W, Zhang X and Luo Y (2024), The impact of high temperature on mechanical properties and behaviors of sandstone.
Front. Earth Sci. 12:1322495.
doi: 10.3389/feart.2024.1322495

The impact of high temperature on mechanical properties and behaviors of sandstone

Juan Jin[1,2]*, Jiandong Liu[1,2], Weixi Chen[3]*, Guoping Li[4], Wei Cheng[1,2], Xiaowen Zhang[1,2] and Yifan Luo[5]

[1]Key Laboratory of Oil & Gas Production, CNPC, Beijing, China, [2]Research Institute of Petroleum Exploration & Development, PetroChina, Beijing, China, [3]Engineering and Technology Department, PetroChina Qinghai Oilfield Company, Dunhuang, China, [4]Drilling & Production Technology Research Institute, PetroChina Qinghai Oilfield Company, Dunhuang, China, [5]School of Civil and Resources Engineering, University of Science and Technology Beijing, Beijing, China

The impact of high temperature environments on the physical and mechanical properties of rocks is a significant factor to consider. The investigation into the impact of elevated temperatures on the physical and mechanical characteristics of rocks holds great importance in the advancement and exploitation of deep-seated mineral reserves, as well as in ensuring the safety and stability of subterranean engineering projects. This study utilizes the state-of-the-art GCTS Mechanical Loading Test System to conduct uniaxial and triaxial compression tests on sandstone after thermal treatment from 25°C to 650°C. In addition, XRD, SEM and nuclear magnetic resonance experiments were carried out on the sandstone after thermal treatment. The aim of the experiments is to provide a quantitative characterization of mechanical properties and behaviors of the rock samples. The results show that the mass, density, and wave velocity of sandstone decrease with increasing temperature, while volume and porosity increase. The mass, volume, and rate of density change of sandstone exhibit a significant increase when subjected to temperatures above 500°C. The uniaxial compressive strength and elastic modulus exhibit an initial increase followed by a subsequent decrease as the temperature rises, with 300°C serving as the critical turning point. The axial peak strain and Poisson's ratio increase with increasing temperature. The cohesion decreases with increasing temperature, while the internal friction angle increases. Additionally, it is observed that the rate of change for both properties exhibits an increase beyond the temperature threshold of 400°C.

KEYWORDS

rock mechanics, high temperature, sandstone, GCTS mechanical loading test system, mechanical property

1 Introduction

The demand for underground mining and construction are increasing with the continuing development of society and economy (Liu et al., 2021; Liu et al., 2022). The continuous exploitation of shallow resources has led to their depletion. Therefore, the development and utilization of deep mineral resources are the most effective and rapid ways to solve the shortage of mineral resources (Xie, 2019; Cai et al., 2021; Cai et al., 2022). In engineering projects such as deep geothermal resource development and utilization, high-temperature radioactive waste disposal, shale gas reservoir thermal fracturing, *in-situ*

FIGURE 1
Rock specimens.

FIGURE 2
KSL-1700X muffle furnace.

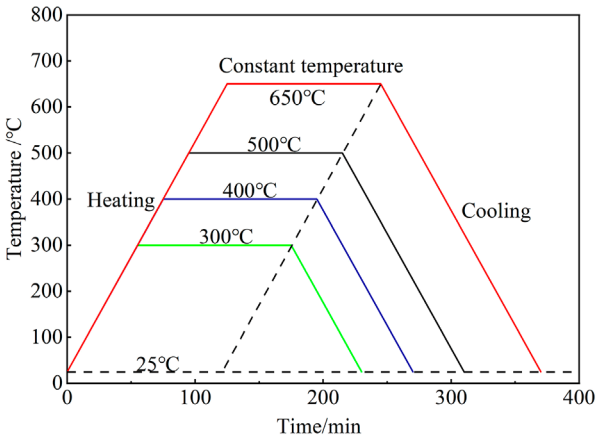

FIGURE 3
Programmed heating path of sandstone.

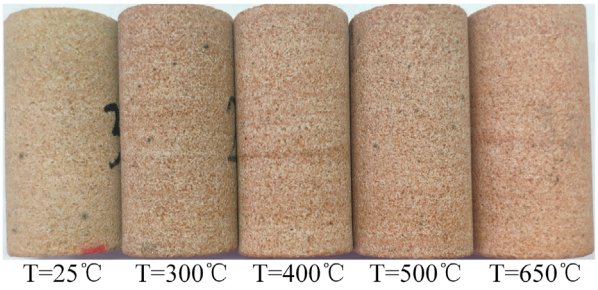

FIGURE 4
Sandstone after different temperature treatments.

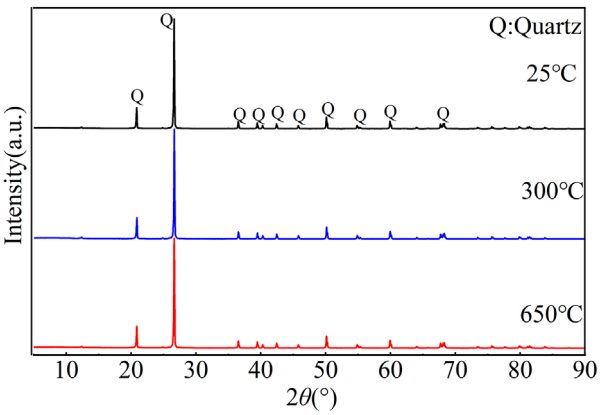

FIGURE 5
XRD spectra of sandstone powder at different temperatures.

gasification and thermal energy transfer of coal and oil shale, ultra-deep well drilling, oil and gas field development, and post-disaster reconstruction of rock underground engineering, rocks may undergo high-temperature heating and cooling. High temperatures can cause changes in the microstructure and mineral composition of rocks, which can affect the strength and deformation characteristics of rocks (Liu et al., 2018; Liu et al., 2020). As a result, the productivity as well as safety stability of the engineering projects may be affected (Luo and Wang, 2011; Sygała et al., 2013; Kong et al., 2016). Therefore, studying the influence of thermal damage on the mechanical properties of rocks is of utmost importance for rock engineering design and the long-term safety evaluation of rock engineering (Ozguven and Ozcelik, 2013; Xu et al., 2022).

Rocks are natural geological materials that are typically considered dual-porosity media, consisting of a mineral matrix and voids (pores and fractures). The physical and mechanical properties of rocks are influenced by the structure and density of pores and fractures (Ma et al., 2021; Ma et al., 2023). The pore and fracture structure of rocks are closely linked to the temperature conditions they experience (Chaki et al., 2008; Yavuz et al., 2010). The impact of high temperatures on the physical and mechanical properties of

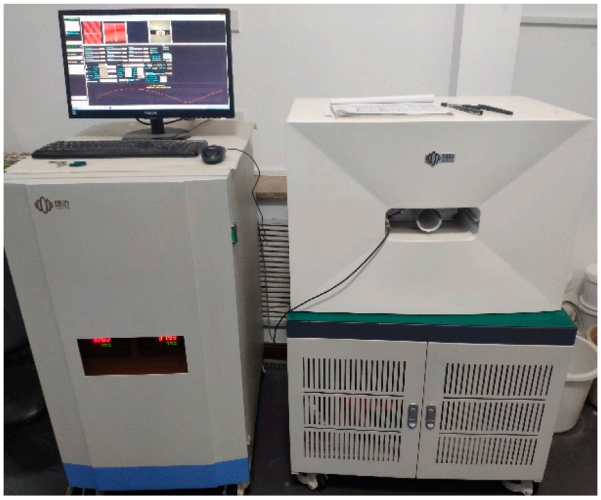

FIGURE 6
MesoMR magnetic resonance imaging analyzer.

rocks has become a significant issue in the fields of rock mechanics and deep earth resource extraction. Many researchers have conducted numerous experimental studies on the impact of high temperatures on the physical and mechanical properties of rocks (Ranjith et al., 2012; Sun et al., 2015; Chen et al., 2017; Xi et al., 2020; Chen et al., 2023; Zhao et al., 2023). Many mechanical properties of rocks, such as strength, elastic modulus, longitudinal wave velocity, cohesion, and internal friction angle, can either increase or decrease with rising temperature (Liang et al., 2006; Chen et al., 2012; Faoro et al., 2016; Sun et al., 2016). Zhang et al. (2022) conducted an experimental study on the mechanical properties of rocks under different cooling methods. The study demonstrates that the sample's deterioration increases gradually as the temperature rises. The peak strength follows a trend of initially increasing and then decreasing with rising temperature. Li et al. (2023) conducted physical and uniaxial compression tests on granite after high-temperature treatment ranging from 25°C to 350°C. The results showed that as the temperature increased, the rate of change in volume, mass, density, longitudinal wave velocity, and porosity of granite also increased. Li and Liu. (2022) studied the physical and mechanical properties of sandstone heat treated from 25° to 800°C. The experimental results showed that when the temperature is lower than 400°C, the physical and mechanical properties of sandstone are not affected, and the failure behavior of sandstone changes from brittleness to ductility with the increase of temperature. Zhao et al. (2017) utilized a polarizing microscope to observe the microstructural alterations in sandstone, granite, and marble following heat treatment at various temperatures. The analysis compared the changes in physical and mechanical properties (such as longitudinal wave velocity, porosity, Young's modulus, peak stress, and corresponding strain) of the three types of rocks during the heat treatment process from room temperature to 800°C, and correlated them with the microstructural change. Yang et al. (2017) conducted uniaxial compression tests on granite to evaluate the effects of high-temperature treatments (200, 300, 400, 500, 600, 700, and 800°C) on crack damage, strength, and deformation failure behavior of the granite. Zhao et al. (2020) conducted research on the changes in the microscopic structure and mechanical properties of a sandstone sample at different temperatures (25°C ~ 900°C) using experimental methods such as nuclear magnetic resonance (NMR), electron microscopy (EM), X-ray diffraction (XRD), and uniaxial compression. It was found that when the temperature exceeds 600 °C, the number of medium and large pores increases rapidly, resulting in a significant increase in permeability and a decrease in the strength of the sandstone. Huang et al. (2023) conducted a study on the effects of real-time high temperature on the mechanical properties of granite. They conducted impact compression tests on granite specimens at temperatures ranging from 20° to 800°C. The results showed that the peak stress of the specimens increased and then decreased with the increase of temperature. It reached a strength threshold at 200°C and then continued to decrease. Chen et al. (2023) conducted triaxial compression experiments on sandstone samples that were subjected to acid corrosion at temperatures of 25, 300, 600, and 900°C. The experimental results showed that the combined effects of chemical damage and thermal damage significantly affected

FIGURE 7
GCTS mechanical loading test system.

various properties of the rock, including mass, density, wave velocity, porosity, uniaxial compressive strength, elastic modulus, and compressive failure characteristics. Kang et al. (2023) utilized the RTX-3000 high-temperature and high-pressure triaxial rock testing machine to perform conventional triaxial compression tests and triaxial unloading confining pressure tests on granite that was heated to 800°C. The objective was to investigate the mechanical properties of thermally treated granite under various rates of unloading confining pressure. Pan et al. (2023) conducted a study on the strength and deformation properties of granite that had been subjected to high temperatures and treated with a chemical solution. This was done through uniaxial compression tests. Based on this, a statistical damage constitutive model was established that considers both the initial thermal-chemical damage and loading damage. The study also discusses the impact of thermal-chemical treatment on the evolution of damage in granite under uniaxial compression.

This research primarily focuses on the impact of high temperatures on different properties of granite. Few studies have been conducted on the evolution of mechanical properties of sandstone after high temperature exposure, and even less research on dense, homogeneous sandstone with fewer mineral impurities.

This article focuses on studying the impact of temperature on sandstone that exhibits good compactness and homogeneity. Heat the sandstone to temperatures of 300°C, 400°C, 500°C, and 650°C, and compare it with specimens at room temperature (25°C). Analyze the influence of high temperature heating on basic physical parameters such as mass, volume, density, and longitudinal wave velocity of sandstone. XRD, SEM and nuclear magnetic resonance experiments were carried out on the sand after thermal treatment. The heat-treated sandstone was subjected to uniaxial and triaxial compression tests using the GCTS-RTR rock triaxial apparatus to obtain the evolution of parameters such as compressive strength, elastic modulus, Poisson's ratio, cohesion, and friction angle with temperature. The study on the evolution of mechanical properties of sandstone with temperature provides a theoretical basis for the extraction of mineral resources in deep sandstone formations and post-disaster engineering construction.

2 Materials and methods

2.1 Sample preparation

To ensure the accuracy of the experimental results, samples were taken from rocks with good appearance structure, compactness, and homogeneity. The rock specimens were all taken from the same rock block to enhance the comparability of the test results. The rock blocks were cored, cut, and polished to obtain standard cylindrical sandstone specimens with a diameter of 25 mm and a height of 50 mm. The specimens meet the requirements of the parallelism of the upper and lower end faces not exceeding 0.05 mm, the diameter deviation of the upper and lower ends not more than 0.1 mm, and the axial deviation less than 0.25°, as shown in Figure 1. We measured the mass, diameter, height, and wave velocity of sandstone at room temperature using an electronic balance, a vernier caliper, and a non-metallic ultrasonic testing analyzer JY-80B. We determined the density and volume from measurement data. In its natural state, the rock sample has an average density of 2.195 g/cm^3, a P-wave velocity of 4188 m/s, and a porosity of 7.65%.

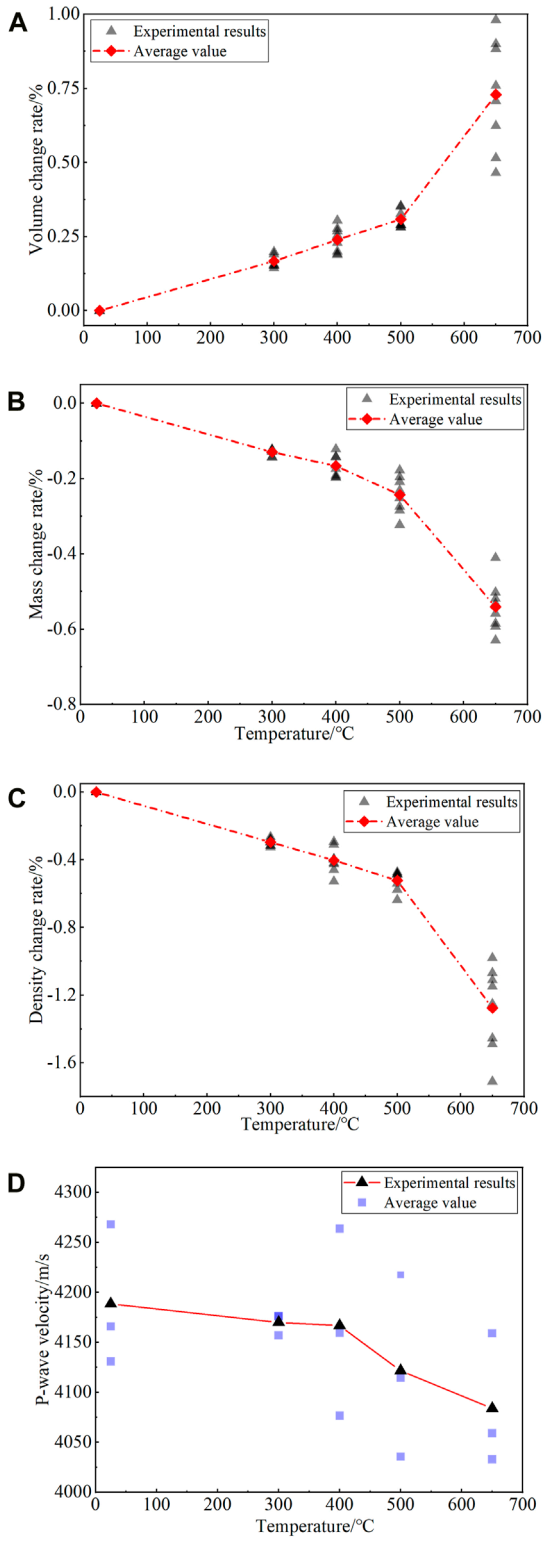

FIGURE 8
The variation of physical parameters of sandstone with temperature. **(A)** Volume. **(B)** Mass. **(C)** Density. **(D)** P-wave velocity.

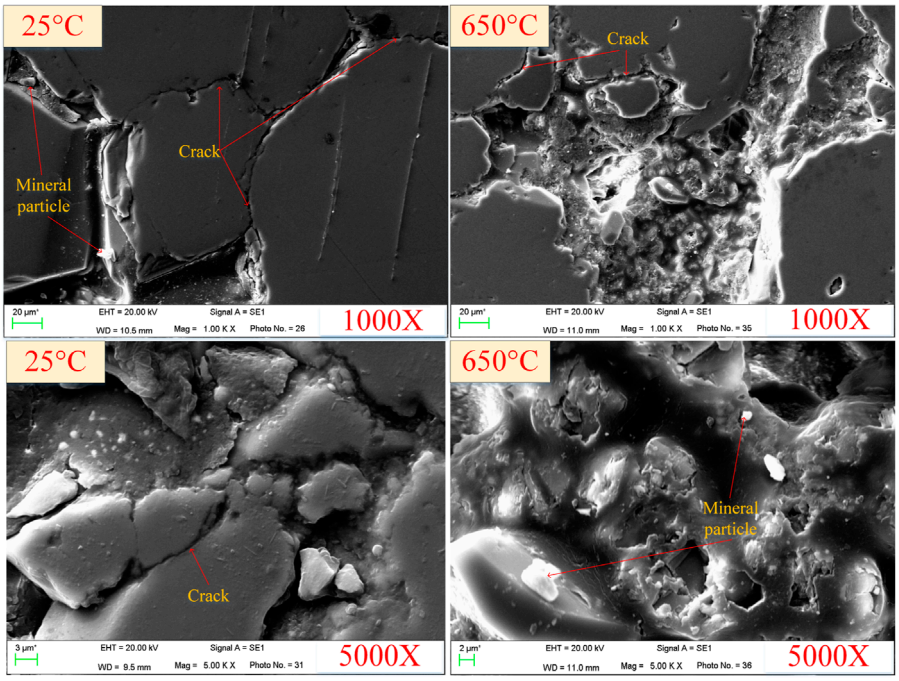

FIGURE 9
SEM images of sandstone microstructure under different heat treatment.

2.2 Thermal treatment

The rock samples were subjected to thermal treatment using a muffle furnace model KSL-1700X (Figure 2). The muffle furnace has a maximum power of 2.5 kW, a maximum working temperature of 1700°C, and a temperature control accuracy of 1°C. The sandstone samples were divided into five groups, and the muffle furnace was used to heat four groups of standard sandstone samples at temperatures of 300°C, 400°C, 500°C, and 650°C, respectively. Before heating, we evenly placed the specimens in the furnace. The heating rate was 5°C/min, with a constant temperature holding time of 2 hours, followed by a cooling rate of 5°C/min (Figure 3). After cooling to room temperature, removed the samples and we measured the mass, dimensions, and P-wave velocity of the specimens. The apparent morphology of rock samples changed at room temperature and after heat treatment (Figure 4). We can be observed that the color of the sandstone gradually deepens from light yellow to orange-yellow with increasing temperature. The surface of the specimens shows an obvious increase in powdery particles and signs of detachment, while the collision sound between the rocks becomes increasingly crisp.

2.3 X-ray diffraction experiment (XRD)

The physical and mechanical properties of rocks at high temperatures are closely related to their mineral composition. By analyzing the mineral composition, we can gain a deeper understanding of the chemical reaction process and the micro-corrosion mechanism. We grinded and sieved three sandstone samples treated at 25°C (room temperature), 300°C, and 650°C. The powder should meet the requirement of 320 mesh. We take 1–2 g of the sample for the XRD experiment. The resulted XRD diffractograms indicate that the sandstone contains almost no other mineral impurities and is predominantly composed of quartz (Figure 5). In addition, we analyzed the XRD pattern and found no change in the intensity of the diffraction peaks.

2.4 Nuclear magnetic resonance experiment

For the rock specimens subjected to high temperatures, a vacuum pressure saturation device was used to perform vacuum pressure saturation for 24 h prior to conducting NMR experiments. The NMR experimental equipment used in this study was the MesoMR magnetic resonance imaging analyzer (Figure 6) with a magnetic field strength of 0.5 ± 0.08T and a main frequency of 21.3 MHz. The diameter of the probe coil was 60 mm. NMR experiments can determine the quantity and distribution of water or other fluids in porous media by measuring the relaxation characteristics of protons in the media. This allows for the analysis of changes in the pore structure of rock samples. NMR analysis enable to were carried out on the four groups of sandstones before heating. Afterwards the four groups of sandstones were heat-treated at high temperatures of 300, 400, 500, and 650°C, respectively, and then,

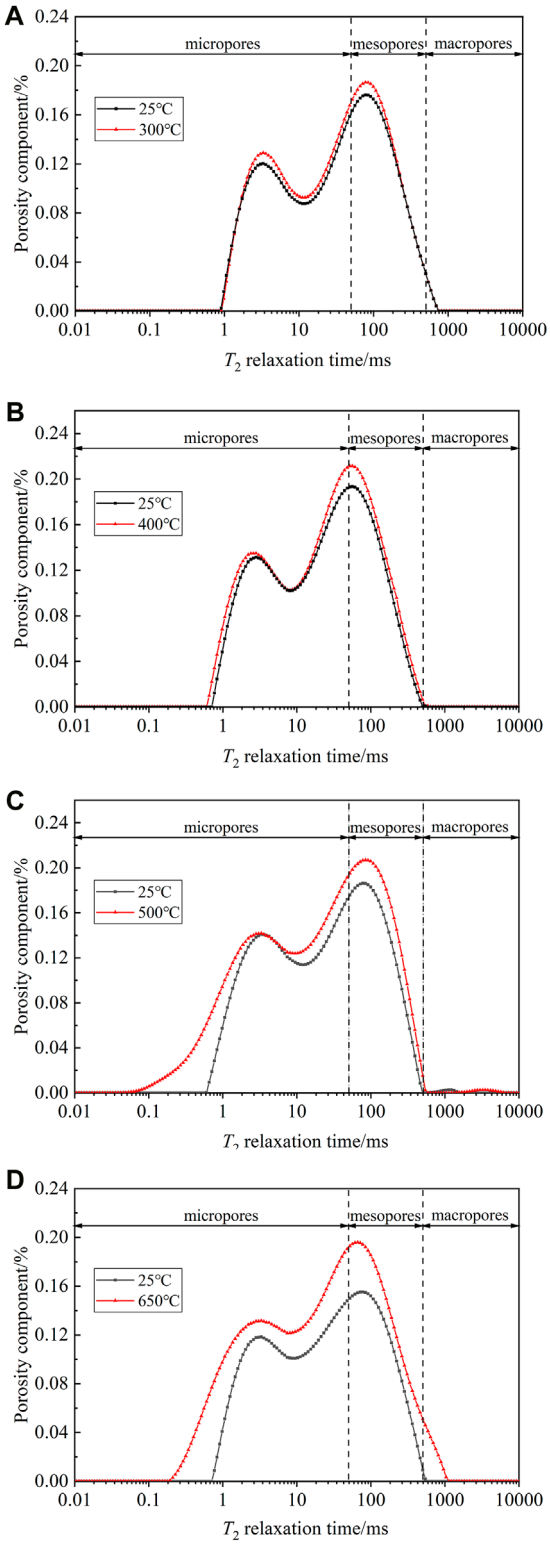

FIGURE 10
Evolution of T_2 relaxation curve after room temperature and heat treatment. **(A)** 300°C. **(B)** 400°C. **(C)** 500°C. **(D)** 650°C.

another set of NMR experiments were carried out to compare the changes in the pore parameters of the sandstones before and after the experiments.

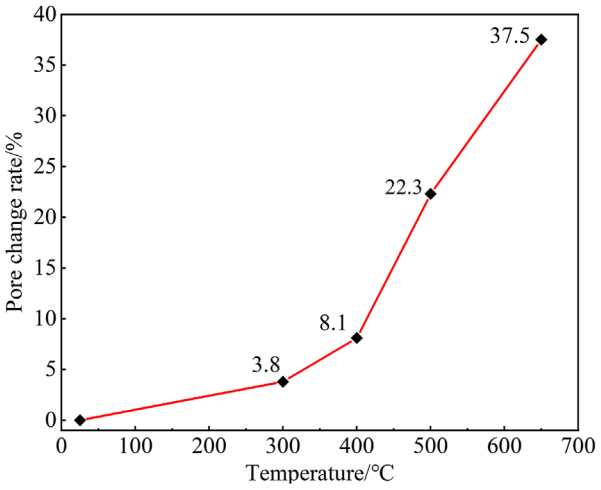

FIGURE 11
The change rate of porosity of sandstone before and after heat treatment.

2.5 Mechanical test

All mechanical tests were conducted on the GCTS Mechanical Loading Test System (GCTS-RTR) (Figure 7). This instrument can perform various tests under different environmental and condition settings, including uniaxial compression tests, uniaxial creep tests, triaxial compression tests under varying confining pressures, permeability tests, dynamic triaxial tests, high-temperature triaxial tests, and ultrasonic velocity measurements. The maximum axial load is 1,500 kN, the maximum confining pressure is 140 MPa, the maximum pore pressure can reach 140 MPa, and the highest operating temperature is 150°C. Sandstone samples at temperatures of 25°C, 300°C, 400°C, 500°C, and 650°C were selected for uniaxial and triaxial compression tests. In the uniaxial compression tests, the axial loading rate was controlled by the percent deformation of the height of the sandstone, which was set at 0.02%/min. The stress-strain curves of sandstone with different heat treatments were obtained during the loading process. In the triaxial compression tests, the confining pressures were set at 10 MPa and 20 MPa, respectively. Before axial compression, the confining pressure was first applied, then, axial compression was performed at a deformation-controlled axial loading rate of 0.025%/min.

3 Results and discussion

3.1 Variation of basic physical parameters

To better represent the variation of volume, mass, and density of rock specimens before and after heating treatment, the volume change rate, mass change rate, density change rate, porosity change rate and P-wave velocity change rate are defined as follows:

$$\eta = \frac{n_a}{n_0} - 1$$

Where η represents the change rate of the parameters; n_0 and n_a represents the value of parameters before and after heating.

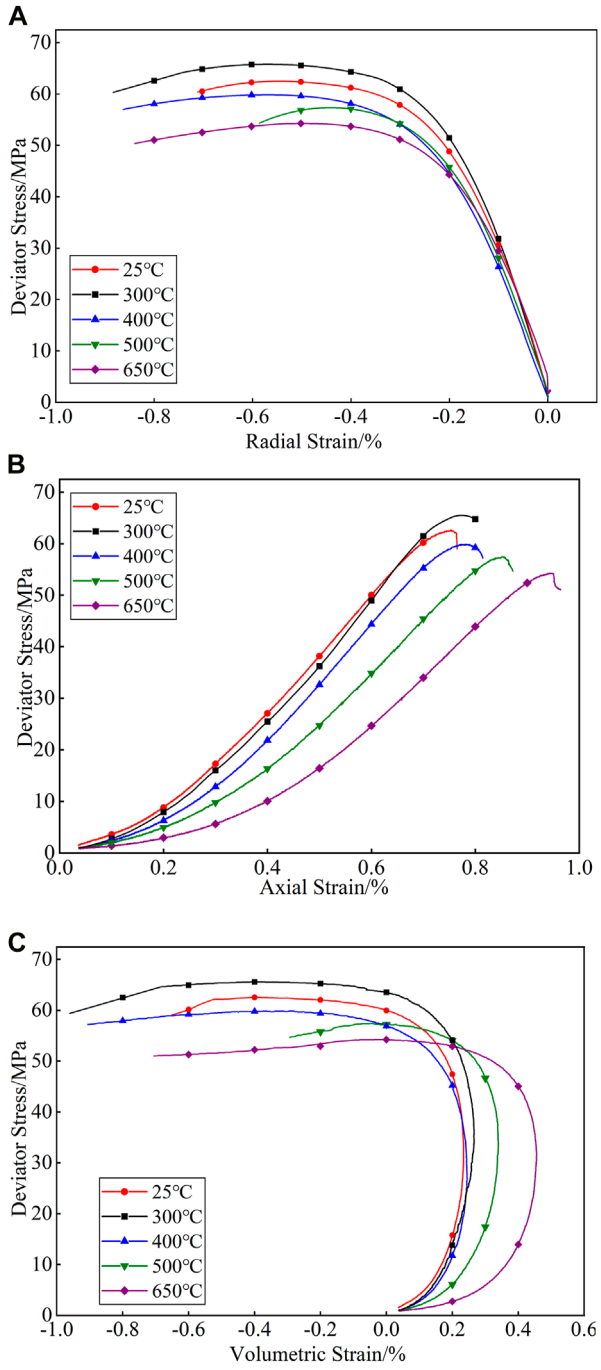

FIGURE 12
Stress–strain curve of sandstone exposed to different temperatures. **(A)** Radial strain. **(B)** Axial strain. **(C)** Volumetric strain.

The changes in the mass, volume, density, and velocity change rate of sandstone specimens after different high-temperature treatments with temperature are shown in Figure 8. By observing the figure, it is evident that the volume of the sandstone specimens increases following high-temperature treatment and further escalates with rising temperatures. At 500°C, the average volume of the sandstone increases by 0.31%. After exceeding 500°C, the growth rate increases significantly, and at 650°C, the volume growth rate is 0.73%. The reason for this phenomenon may be that the high temperature causes thermal expansion of the mineral particles in the sandstone, resulting in irreversible deformation (Dong et al., 2022). After exceeding 500°C, some mineral crystals undergo a phase transformation, and quartz grains transform from the α phase to the β phase at 573°C, as shown by the observation result of SEM (Figure 9). Microfracture expansion or new cracks are generated, resulting in a rapid increase in the volume of the sandstone specimens (Su et al., 2022). The mass decreases with the increase in temperature, as shown in Figure 8B. As the heating process progresses, the weakly bound water inside the rock continuously evaporates. At 500°C, the mass decreases by 0.24%, and there is a slight acceleration in mass loss after exceeding 500°C, with a mass reduction of 0.54% at 650°C. This may be due to the decomposition of a small amount of internal minerals in the rock and the evaporation of strongly bound water (Lei et al., 2019). Due to the increase in volume and decrease in mass, the density decreases with the increase in temperature, with a decrease of 1.28% at 650°C. The P-wave velocity of the specimen decreases as the temperature rises, albeit the change is relatively minor overall. From 25°C to 650°C, the P-wave velocity of the sandstone specimen decreased from 4,188 m/s to 4,084 m/s, resulting in a decrease of 2.5%.

3.2 Porosity of sandstone after heat treatment

The nuclear magnetic resonance analysis of porous media such as rocks involves using the CPMG pulse sequence under fully saturated conditions to measure the transverse relaxation time T_2. By analyzing the changes in T_2 spectrum, the number and size distribution of pores in the rock sample can be determined. This device is used to measure the porosity, transverse relaxation time T_2 spectrum, and changes in pore size distribution of rock specimens before and after heat treatment. The alteration in rock porosity, both pre- and post-heating, exhibits a positive correlation with the peak value of the T_2 spectrum. A higher peak value corresponds to a greater number of pores of the corresponding size. The position of the T_2 spectrum peak on the relaxation time axis is directly proportional to the pore radius. In other words, a higher T_2 value indicates a larger pore radius. Typically, the rock pores are categorized into micropores (<1 μm), mesopores (1–10 μm), and macropores (>10 μm) based on their respective sizes. Based on the relationship between relaxation time calculated by the NMR analyzer and pore size distribution, micropores are identified as those with relaxation times less than 50 ms, mesopores fall within the range of 50 ms–500 ms, and macropores are characterized by relaxation times exceeding 500 ms. The experimental results before and after heating are shown in Figure 10, revealing that the development of pores occurs gradually as the temperature increases. Below 500°C, there is a gradual formation of micropores and mesopores, accompanied by a slow increase in porosity. Post 500°C, there is rapid formation of micropores and mesopores, and at 650°C, macropores increase in the rock, resulting in a rapid increase in total porosity. The variation rate of sandstone porosity before and after heat treatment is depicted in Figure 11. Overall, porosity increases with temperature, with the rate of change significantly accelerating after reaching 400°C. At 650°C,

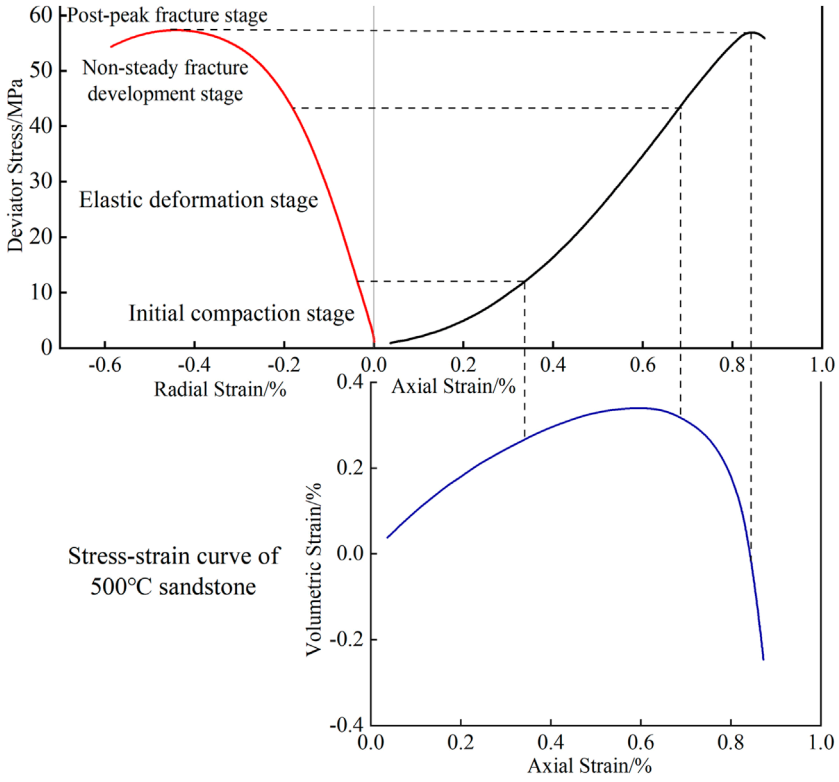

FIGURE 13
The fracture process of heat-treated sandstone specimens.

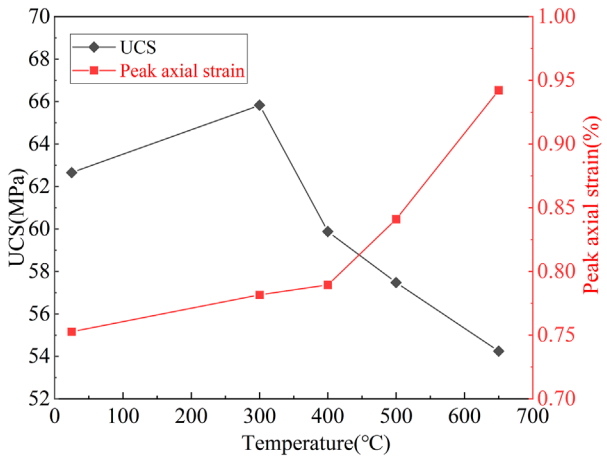

FIGURE 14
Axial peak strain and UCS of sandstone after heat treatment.

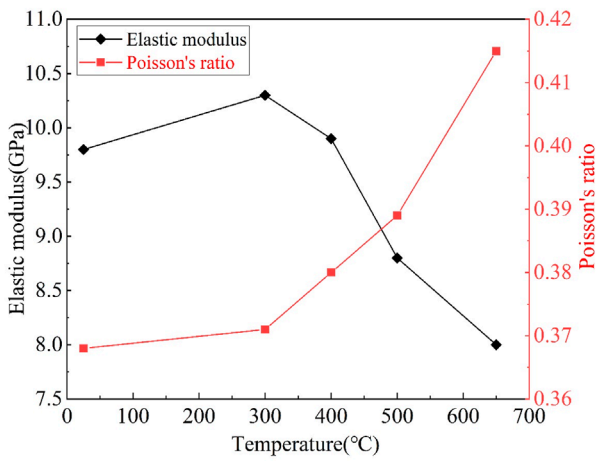

FIGURE 15
Elastic modulus and Poisson's ratio of sandstone after heat treatment.

porosity increases by 37.5%. Before reaching a temperature of 400°C, the main changes in sandstone include the volatilization of water components and the initiation of microcracks. When the temperature exceeds 400°C, there is an increase in macropores pores and interconnected pores, as well as a significant increase in total porosity.

3.3 Mechanical properties of sandstone after high-temperature heating

We conducted uniaxial and triaxial compression tests on the sandstone specimens after heat treatment. Figure 12 shows the stress-strain curves of sandstone samples under uniaxial

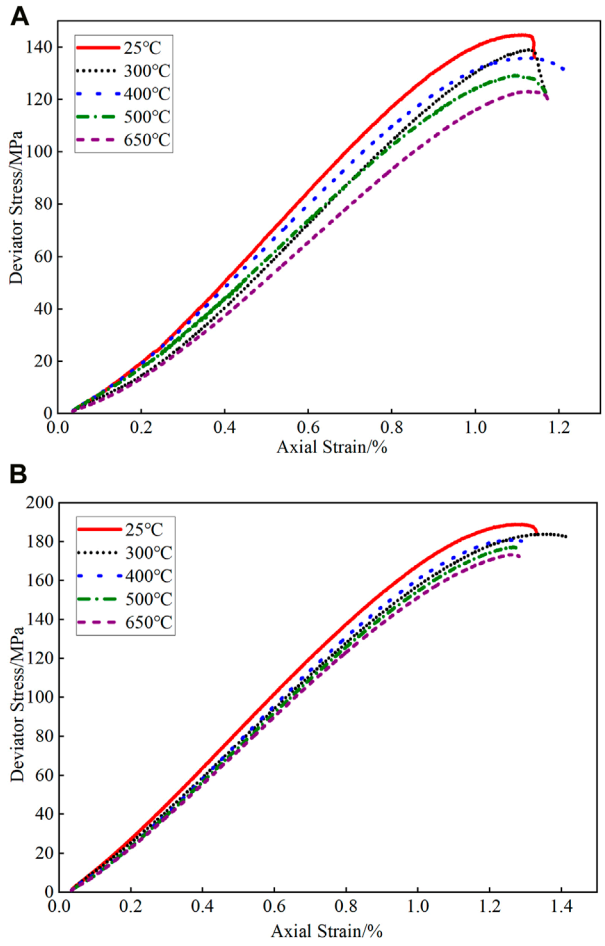

FIGURE 16
Stress-strain curves of rock after heat treatment under different confining pressures. **(A)** 10 MPa. **(B)** 20 MPa.

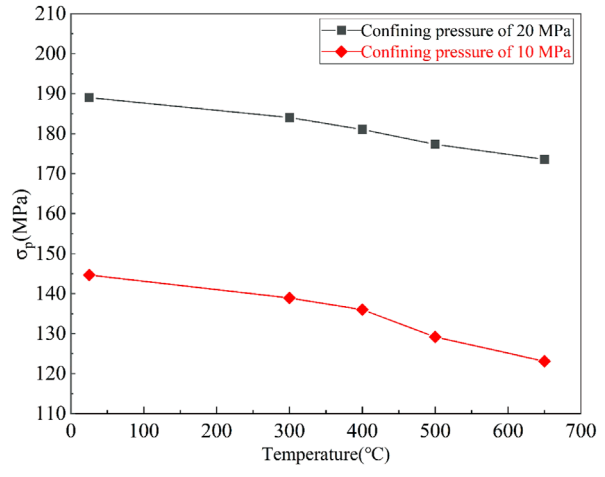

FIGURE 17
Peak stress in triaxial compression test of sandstone after heat treatment.

compression at different temperatures. The peak stress, axial peak strain, elastic modulus and Poisson's ratio of sandstone are obtained from the peak and slope of the curve.

The deformation stage of heat-treated sandstone specimens can be divided into four stages: the initial compaction stage, the elastic deformation stage, the non-steady fracture development stage, and the post-peak fracture stage, as shown in Figure 13. At the initial compaction stage, the original cracks inside the rock specimen are compacted under the action of external load, to produce crack closure, and the slope of the curve gradually increases as the external load continues to increase. During the elastic deformation stage, the stress-strain curve of the rock is approximately linear, and the deformation of the rock follow similar trends as the applied stress. During the non-steady fracture development stage, the continuous increase of external load leads to the formation of new cracks appear the rock specimen that extend in different directions until the specimen loses its bearing capacity and fails. The post-peak fracture stage is characterized by the damaging of the internal structure of the rock specimens after the bearing capacity of the rock reaches the peak strength. Moreover, the bearing capacity of the specimen rapidly decreases with the increase of deformation.

The variation of uniaxial compressive strength (UCS) and axial peak strain of sandstone at different temperatures is shown in Figure 14. The UCS of sandstone increases from 62.66 MPa to 65.83 MPa, with a growth rate of 4.8%, as the temperature rises from 25°C to 300°C. However, the UCS of sandstone decreases rapidly with the increase in temperature from 300°C to 650°C, and at 650°C, it decreases to 54.25 MPa, which is a 13.4% reduction compared to the sandstone at room temperature. This may be due to the expansion of rock particles caused by high temperatures below 300°C, leading to the closure of micropores and microcracks, resulting in an increase in the strength of the sandstone specimens. However, after 300°C, the development of micropores and microcracks within the rock rapidly reduces its strength (Sirdesai et al., 2019). The peak strain gradually increases with the increase in temperature, from 0.75% to 0.94%. The increase in peak strain is slow from 25°C to 400°C, but it increases rapidly from 400°C to 650°C.

The elastic modulus and Poisson's ratio can be used to measure the ability of granite to deform under stress. The elastic modulus and Poisson's ratio of rock samples can be determined during the elastic deformation stage. The elastic modulus is the ratio of the change in axial stress to the change in axial strain, while Poisson's ratio is defined as the ratio of the change in radial strain to the change in axial strain. The variation of the elastic modulus and Poisson's ratio of sandstone at different temperatures is shown in Figure 15. The elastic modulus of sandstone increases from 9.8 GPa to 10.3 GPa with a growth rate of 5.1% as the temperature rises from 25°C to 300°C. Beyond 300°C, the elastic modulus gradually decreases as the temperature increases. At 650°C, the elastic modulus is 8.0 GPa with a reduction rate of 18.4%, which exhibits a similar trend as the uniaxial compressive strength. Generally, Poisson's ratio increases with increasing temperature. At room temperature, the Poisson's ratio is initially 0.368. The rate of change of Poisson's ratio gradually increases with temperature, reaching 0.415 at 650°C, increasing by 12.8%.

The cohesion and internal friction angle are two important mechanical parameters of rocks, which can be obtained through the

TABLE 1 Parameters of the principal stress.

Temperature (°C)	σ_1 (MPa)	σ_3 (MPa)	σ_1' (MPa)	σ_3' (MPa)
25	10	144	20	189
300	10	138	20	184
400	10	135	20	181
500	10	129	20	177
650	10	123	20	173

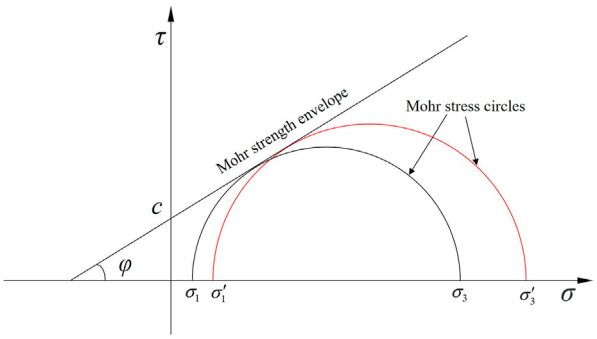

FIGURE 18
Mohr stress circles and Mohr Strength Envelope.

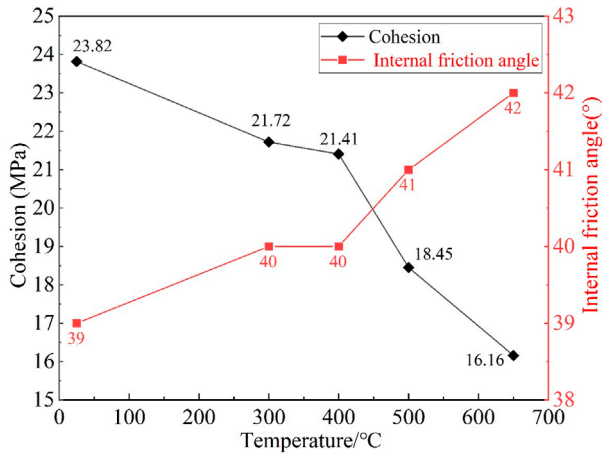

FIGURE 19
Cohesion and internal friction angle of sandstone after heat treatment.

equation of Mohr-Coulomb criterion as follows:

$$\frac{1}{2}(\sigma_1 - \sigma_3) = c\cos\varphi + \frac{1}{2}(\sigma_1 + \sigma_3)\sin\varphi$$

Where σ_1 and σ_3 represent the minimum and maximum principal stresses respectively; c represents the cohesive strength of the rock; φ represents the internal friction angle of the rock.

The results of the triaxial compression test are shown in Figure 16. Base on the experimental results, peak stress in triaxial compression test of sandstone after heat treatment were calculated and reported in Figure 17. In addition, we sorted out the principal stress related parameters as shown in Table 1. The difference between the maximum principal stress and the minimum principal stress at each level of confining pressure is taken as the diameter, and the average value of the maximum principal stress and the minimum principal stress is taken as the center to draw the Mohr stress circles. The tangent line of the Mohr stress circles is the Mohr strength envelope. The intercept of the tangent line on the y-axis is cohesion, and the angle between the tangent line and the positive direction of the x-axis represents the internal friction angle, as shown in Figure 18.

Figure 19 shows the variation of cohesion and internal friction angle with temperature. Overall, the cohesion decreases with increasing temperature. Between 25°C and 400°C, cohesion slowly decreases from 23.82 MPa to 21.41 MPa. The rate of decrease in cohesion accelerates between 400°C and 650°C, and at 650°C, cohesion is only 16.16 MPa, a decrease of 32.2%. On the other hand, the internal friction angle increases with increasing temperature. At room temperature, the internal friction angle is 39°, while at 650°C, it is 42°, increasing by 7.7%. Compared to cohesion, the change in internal friction angle is relatively slow.

4 Conclusion

The sandstone samples are light yellow at room temperature, and as the heat treatment temperature increases, the color gradually deepens and becomes orange-yellow. The sound of the rocks colliding becomes crisper. Additionally, the surface particles increase and there is phenomenon of powder shedding.

Through XRD experiments, it was discovered that the main component of sandstone is quartz (SiO2). Other mineral contents are extremely low, and after being heated to 650°C, there is no change in the mineral composition.

The mass and density of sandstone decrease with increasing temperature, while the volume increases. The rate of change of these three parameters experiences a significant increase when the temperature surpasses 500°C. The P-wave velocity decreases with increasing temperature, but the magnitude of change is relatively small. The porosity of sandstone increases with increasing temperature, and when the temperature exceeds 400°C, the porosity increases sharply.

Through the GCTS mechanical testing system, the uniaxial compressive strength, axial peak strain, deformation modulus, Poisson's ratio, cohesion, and internal friction angle of sandstone were obtained. The uniaxial compressive strength and elastic modulus of sandstone first increase and then decrease when increasing from 25°C to 650°C, and an inflection point occurs at 300°C. The axial peak strain and Poisson's ratio increase with increasing temperature. Cohesion decreases with increasing temperature, while the internal friction angle increases. When the temperature surpasses 400°C, there is an escalation in the rate of alteration for both cohesion and internal friction angle.

Data availability statement

The original contributions presented in the study are included in the article/supplementary material, further inquiries can be directed to the corresponding authors.

Author contributions

JJ: Conceptualization, Formal Analysis, Funding acquisition, Methodology, Project administration, Resources, Supervision, Visualization, Writing–original draft. JL: Conceptualization, Methodology, Writing–original draft. WxC: Data curation, Formal Analysis, Writing–original draft. GL: Software, Validation, Writing–original draft. WCg: Software, Supervision, Validation, Writing–original draft. XZ: Conceptualization, Funding acquisition, Methodology, Writing–original draft. Yifan Luo: Writing–review and editing.

Funding

The author(s) declare financial support was received for the research, authorship, and/or publication of this article.

Conflict of interest

Authors JJ, JL, WCg, and WZ were employed by CNPC. Authors JJ, JL, WCg, and XZ were employed by PetroChina. Author WxC was employed by PetroChina Qinghai Oilfield Company. Author GL was employed by PetroChina Qinghai Oilfield Company.

The remaining author declares that the research was conducted in the absence of any commercial or financial relationships that could be construed as a potential conflict of interest.

The author(s) declare financial support was received for the research, authorship, and/or publication of this article. This research was funded by Study on the evolution law of mineral structure and rock mechanical properties under ultra-high temperature conditions (Project Number: 2022-KFKT-02, PetroChina RIPED). The funder had the following involvement in the study: study design, data collection, provision of experimental equipment, decision to submit it for publication.

Publisher's note

References

Cai, M., Dor, J., Chen, X., Mao, J., Tang, C., Liu, Z., et al. (2021). Development strategy for Co-mining of the deep mineral and geothermal resources. *Stud. CAE.* 23 (6), 43–45. doi:10.15302/J-SSCAE-2021.06.006

Cai, M., Ma, M., Pan, J., Xi, X., and Guo, Q. (2022). Co-mining of mineral and geothermal resources: a state-of-the-art review and future perspectives. *Chin. J. Eng.* 44 (10), 1669–1681. doi:10.13374/j.issn2095-9389.2022.08.24.001

Chaki, S., Takarli, M., and Agbodjan, W. (2008). Influence of thermal damage on physical properties of a granite rock: porosity, permeability and ultrasonic wave evolutions. *Constr. Build. Mat.* 22 (7), 1456–1461. doi:10.1016/j.conbuildmat.2007.04.002

Chen, G., Li, Y., Li, T., and Zhang, G. (2023a). Experimental study on the mechanical properties of intermittent jointed sand-stone considering water-rock interaction and confining pressure effect. *Bull. Eng. Geol. Environ.* 82 (4), 113. doi:10.1007/s10064-023-03156-w

Chen, Q., Chen, Y., Xiao, P., Du, X., Pan, Y., and Azzam, R. (2023b). Mechanical properties and damage constitutive model of sandstone after acid corrosion and high temperature treatments. *Int. J. Min. Sci. Technol.* 33 (06), 747–760. doi:10.1016/j.ijmst.2022.11.011

Chen, S., Yang, C., and Wang, G. (2017). Evolution of thermal damage and permeability of Beishan granite. *Appl. Therm. Eng.* 110, 1533–1542. doi:10.1016/j.applthermaleng.2016.09.075

Chen, Y., Ni, J., Shao, W., and Azzam, R. (2012). Experimental study on the influence of temperature on the mechanical properties of granite under uniaxial compression and fatigue loading. *Int. J. Rock Mech. Min. Sci.* 56, 62–66. doi:10.1016/j.ijrmms.2012.07.026

Dong, Z., Chen, Y., Wang, X., Kong, L., Wang, L., Li, X., et al. (2022). Evaluation of thermophysical and mechanical properties of sandstone due to high-temperature. *Materials* 15 (23), 8692. doi:10.3390/ma15238692

Faoro, I., Elsworth, D., and Candela, T. (2016). Evolution of the transport properties of fractures subject to thermally and mechanically activated mineral alteration and redistribution. *Geofluids* 16 (3), 396–407. doi:10.1111/gfl.12157

Huang, Y., Qu, L., Li, Y., Zhai, Y., and Xie, Y. (2023). Mechanical properties of granite under impact compression after re-al-time high temperature. *Explos. Shock Waves* 43 (02), 62–75. doi:10.11883/bzycj-2022-0196

Kang, P., Jing, Z., Hao, L., Gao, X., and Zheng, C. (2023). Mechanical properties of thermally treated granite subjected to different multi-stage unloading paths. *Environ. Earth Sci.* 82 (1), 53. doi:10.1007/s12665-022-10656-7

Kong, B., Wang, E., Li, Z., Wang, X., Liu, J., and Li, N. (2016). Fracture mechanical behavior of sandstone subjected to high-temperature treatment and its acoustic emission characteristics under uniaxial compression conditions. *Rock Mech. Rock Eng.* 49 (12), 4911–4918. doi:10.1007/s00603-016-1011-3

Lei, R., Wang, Y., Zhang, L., Liu, B., Long, K., Luo, P., et al. (2019). The evolution of sandstone microstructure and mechanical properties with thermal damage. *Energy Sci. Eng.* 7 (6), 3058–3075. doi:10.1002/ese3.480

Li, F., Li, C., He, H., Yang, B., and Lu, J. (2023). Research on physical-mechanical properties and energy evolution characteristics of granite after high temperature treatment. *Therm. Sci.* 27 (1B), 497–504. doi:10.2298/TSCI220827009L

Li, M., and Liu, X. (2022). Effect of thermal treatment on the physical and mechanical properties of sandstone: insights from experimentsand

simulations. *Rock Mech. Rock Eng.* 55, 3171–3194. doi:10.1007/s00603-022-02791-1

Liang, W., Xu, S., and Zhao, Y. (2006). Experimental study of temperature effects on physical and mechanical characteristics of salt rock. *Rock Mech. Rock Eng.* 39 (5), 469–482. doi:10.1007/s00603-005-0067-2

Liu, L., Ji, H., Elsworth, D., Zhi, S., Lv, X., and Wang, T. (2020). Dual-damage constitutive model to define thermal damage in rock. *Int. J. Rock Mech. Min. Sci.* 126, 104185. doi:10.1016/j.ijrmms.2019.104185

Liu, L., Ji, H., Lü, X., Wang, T., Zhi, S., Pei, F., et al. (2021). Mitigation of greenhouse gases released from mining activities: a review. *Int. J. Min. Metall. Mater* 28, 513–521. doi:10.1007/s12613-020-2155-4

Liu, L., Zhang, L., and Ji, H. (2022). Mechanism analysis of rock damage and failure based on the relation between deep chamber axial variation and *in situ* stress fields. *Chin. J. Eng.* 44 (4), 516–525. doi:10.13374/j.issn2095-9389.2021.04.09.003

Liu, L., Zhu, W., Wei, C., Elsworth, D., and Wang, J. (2018). Microcrack-based geomechanical modeling of rock-gas interaction during supercritical CO2 fracturing. *J. Pet. Sci. Eng.* 164, 91–102. doi:10.1016/j.petrol.2018.01.049

Luo, J., and Wang, L. (2011). High-temperature mechanical properties of mudstone in the process of underground coal gasification. *Rock Mech. Rock Eng.* 44 (6), 749–754. doi:10.1007/s00603-011-0168-z

Ma, T., Jiang, L., Shen, W., Cao, W., Guo, C., and Nick, H. (2023). Fully coupled hydro-mechanical modeling of two-phase flow in deformable fractured porous media with discontinuous and continuous Galerkin method. *Comput. Geotech.* 164, 105823. doi:10.1016/j.compgeo.2023.105823

Ma, T., Zhang, K., Shen, W., Guo, C., and Xu, H. (2021). Discontinuous and continuous Galerkin methods for compressible single-phase and two-phase flow in fractured porous media. *Adv. Water Resour.* 156, 104039. doi:10.1016/j.advwatres.2021.104039

Ozguven, A., and Ozcelik, Y. (2013). Investigation of some property changes of natural building stones exposed to fire and high heat. *Constr. Build. Mat.* 38 (2), 813–821. doi:10.1016/j.conbuildmat.2012.09.072

Pan, J., Zhang, Y., Li, P., Wu, X., and Xi, X. (2023). Mechanical properties and thermo-chemical damage constitutive model of granite subjected to thermal and chemical treatments under uniaxial compression. *Constr. Build. Mat.* 390, 131755. doi:10.1016/j.conbuildmat.2023.131755

Ranjith, P., Viete, D., Chen, B., Samintha, M., and Perera, A. (2012). Transformation plasticity and the effect of temperature on the mechanical behaviour of Hawkesbury sandstone at atmospheric pressure. *Eng. Geol.* 151, 120–127. doi:10.1016/j.enggeo.2012.09.007

Sirdesai, N., Mahanta, B., Ranjith, P., and Singh, T. (2019). Effects of thermal treatment on physico-morphological properties of Indian fine-grained sandstone. *Bull. Eng. Geol. Environ.* 78, 883–897. doi:10.1007/s10064-017-1149-6

Su, H., Nie, Y., Feng, Y., Yu, L., Chen, G., and Wang, W. (2022). Experimental investigation on microstructure characteristics and deformation failure behaviors of sandstone after high temperature under Brazilian splitting. *Geomech. Geophys. Geo-Energy Geo-Resour.* 8 (4), 121. doi:10.1007/s40948-022-00429-8

Sun, Q., Lu, C., Cao, L., Li, W., Geng, J., and Zhang, W. (2016). Thermal properties of sandstone after treatment at high temperature. *Int. J. Rock Mech. Min. Sci.* 85, 60–66. doi:10.1016/j.ijrmms.2016.03.006

Sun, Q., Zhang, W., Xue, L., Zhang, Z., and Su, T. (2015). Thermal damage pattern and thresholds of granite. *Environ. Earth Sci.* 74, 2341–2349. doi:10.1007/s12665-015-4234-9

Sygała, A., Bukowska, M., and Janoszek, T. (2013). High temperature versus geomechanical parameters of selected rocks-the present state of research. *J. Sustain. Min.* 12 (4), 45–51. doi:10.7424/jsm130407

Xi, B., Wu, Y., and Wang, S. (2020). Experimental study on mechanical properties of granite taken from Gonghe basin, Qinghai province after high temperature thermal damage. *Chin. J. Rock Mech. Eng.* 39 (1), 69–83. doi:10.13722/j.cnki.jrme.2019.0182

Xie, H. (2019). Research review of the state key research development program of China: deep rock mechanics and mining theory. *J. China Coal Soc.* 44 (5), 1283–1305. doi:10.13225/j.cnki.jccs.2019.6038

Xu, X., Yue, C., and Xu, L. (2022). Thermal damage constitutive model and brittleness *index Based on energy Dissipation for deep rock. Math. Math. (Basel).* 10 (3), 410. doi:10.3390/math10030410

Yang, S., Ranjith, P., Jing, H., Tian, L., and Ju, Y. (2017). An experimental investigation on thermal damage and failure mechanical behavior of granite after exposure to different high temperature treatments. *Geothermics* 65, 180–197. doi:10.1016/j.geothermics.2016.09.008

Yavuz, H., Demirdag, S., and Caran, S. (2010). Thermal effect on the physical properties of carbonate rocks. *Int. J. Rock Mech. Min. Sci.* 47 (1), 94–103. doi:10.1016/j.ijrmms.2009.09.014

Zhang, J., Lu, Y., Pang, J., and Bu, Y. (2022). Experimental study on mechanical properties of high temperature granite with different cooling methods. *Appl. Sci.* 12, 5968. doi:10.3390/app12125968

Zhao, C., Ma, Q., Sun, X., and Su, H. (2023). Research progress of thermal damage mechanical properties of high-temperature rocks. *Water Sci. Technol. Econ.* 29 (01), 8–13. doi:10.3969/j.issn.1006-7175.2023.01.002

Zhao, Y., Wei, K., Zhou, J., Li, X., and Chen, Y. (2017). Laboratory study and micromechanical analysis of mechanical behaviors of three thermally damaged rock. *Chin. J. Rock Mech. Eng.* 36 (01), 142–151. doi:10.13722/j.cnki.jrme.2015.1750

Zhao, Y., Wu, C., Jin, A., and Sun, H. (2020). Experimental study of sandstone microstructure and mechanical properties under high temperature. *Soils Rocks* 41 (07), 2233–2240. doi:10.16285/j.rsm.2019.1436